

## Potential of *Carica Papaya* Stem Activated Carbon in Removal of Undesired Compounds from Metakaolin

Ezekiel Adeyemi Adetoro<sup>1,\*</sup>, Rasheed Abdulwahab<sup>2</sup>, Omolara Dasola Adetoro<sup>3</sup>, Folahan Okeola Ayodele<sup>4</sup>, Taofeek Olalekan Ajijola<sup>5</sup> and Benjamin Ayowole Alo<sup>6</sup>

<sup>1</sup>Department of Civil Engineering, Olabisi Onabanjo University, Ago-Iwoye, Nigeria

<sup>2</sup>Department of Civil Engineering, University of South Africa, Johannesburg, South Africa

<sup>3</sup>Department of Food Science, Ladoke Akintola University of Technology, Ogbomosho, Nigeria

<sup>4</sup>Department of Civil Engineering, Federal Polytechnic, Ado-Ekiti, Nigeria

<sup>5</sup>Eljay Consult and Constructing Limited, Lagos, Nigeria

<sup>6</sup>Department of Civil Engineering, Ekiti State University, Ado-Ekiti, Nigeria

(\*Corresponding author's e-mail: [yemmieadyt@yahoo.com](mailto:yemmieadyt@yahoo.com))

Received: 2 September 2023, Revised: 19 September 2023, Accepted: 11 October 2023, Published: 15 February 2024

### Abstract

Metakaolin (MK) is a pozzolan exhibiting additional cementitious tendency and is made by dehydroxylating Kaolin Clay (KC). In this study, potential of *Carica papaya* Stem Activated Carbon (CPSAC) in removal of undesired compounds or impurities from MK was examined. *Carica papaya* Stem (CPS) was processed into powder and chemically activated using hydrochloric (HCl) acid, while MK was produced from KC through calcination process. Five conical flasks contained 5 to 25 % CPSAC at 5 % weight intervals. Two hundredg of MK or KC was added and well mixed to achieve homogeneity. The KC+CPSAC samples were subjected to calcination inside a muffle furnace at 700 °C and removed after 1 to 2 h then allowed to cool; while the MK+CPSAC samples were soaked in water (125 mL for each sample) for 24 h, thereafter oven-dried at 105 °C. Subsequently, the samples obtained were subjected to Scanning Electron Microscopy (SEM) analysis to investigate their surface morphology, while X-Ray Diffraction (XRD) and X-Ray Fluorescence (XRF) techniques were employed to ascertain their chemical and mineralogical compositions, respectively. The data obtained from chemical composition analyses were thereafter subjected to optimization studies. The SEM plates showed that the sizes of all the samples were within ranges of 2 and 50 nm, and their intensity pinnacles from XRD plots ranged between 200 and 4000 cps. CPSAC (21.42%) eliminated the unwanted compounds in the MK and increased the amount of its major oxides (Al<sub>2</sub>O<sub>3</sub>, CaO, SiO<sub>2</sub> and Fe<sub>2</sub>O<sub>3</sub> by 43.76, 16.89, 12.76, 6.51 %, respectively). In conclusion, CPSAC showed potential as a viable industrial treatment material for MK.

**Keywords:** Activated carbon, Calcination process, *carica papaya* stem, Kaolin clay, Metakaolin

### Introduction

MK is a kind of pozzolan that demonstrates enhanced cementitious behaviour. An amorphous aluminate silicate is formed when KC is dehydroxylated at temperatures between 500 and 800°C [1-4]. KC is a naturally occurring granular white rock that is rich in hydrated aluminium silicate and is characterized by the mineral kaolinite. Possible causes of its whiteness include a low iron concentration and the presence of contaminants in its original formation. Because of the proportions of its constituent elements - silicon dioxide, aluminium oxide and water - kaolinite has a pseudo-flaky, earthy fracture pattern and is hexagonal. KC is found in some states of Nigeria (including Abia, Bauchi, Borno, Delta, Edo, Ekiti, Kaduna, Kano, Kogi, Nassarawa, Niger, Ogun, Oyo, Plateau and Sokoto), some other Africa countries, America, China, India etc. The categorization of clay is based on the constituent minerals, which can be classified into 4 distinct classes: Kaolinite, halloysite, nacrite and dickite. The composition comprises additional minerals, namely attapulgite, feldspar, bauxite, rutile, quartz, mica, illite and sillimanite [2,5,6].

Previous studies have focused on investigating the impact of MK and various substances, including blast furnace slag [19], cement and lime powder [7], cement and coal bottom ash [8], eggshell powder [9], nanosilica [1], sugar cane bagasse and millet husk ash [10], treated rice husk ash [5] and other materials, on the efficacy of concrete. A comprehensive review of MK was published by [2,11,12]. Alumina particles extracted from inexpensive kaolinite have been reported by [13] using calcination at 700 °C with

sodium chloride and leaching with sulphuric and HCl acid. The above reviewed works and others showed that MK, which is generated from KC found in nature, has been extensively employed as a cement substitute in the production of mortar and concrete, although the impact of the clay source on MK's reactivity and pozzolanic properties has received little study [1].

The issue of impurities or undesired compounds within MK is a significant concern that has yet to be adequately resolved. The conventional approach for eliminating undesired compounds from MK involves calcination, although it may not be entirely effective in removing all such compounds [2,12]. Thus, prompt the need to look into effect(s) of Activated Carbon (AC) on pozzolanic properties of MK. Previous research works indicated that AC has binding ability due to presence of some functional ligands or metabolites, which could help in remediating some metals or compounds from soil, water and any other medium [6,14]. Due to its limited availability, using commercial AC for research purposes is always costly. Therefore, the AC used in this investigation was derived from a locally available agricultural biomaterial i.e. CPS. Literature is very scarce on the ability of AC to remove impurities or undesired compounds from MK, though in the recent past, [6] showed possibility of treatment effects on reactivity of MK using AC (i.e. *Azadirachta indica* bark AC (AIBAC)) - 16.22% of AIBAC removed unwanted compounds from MK totally.

AC produced locally from agricultural biomaterials have the potential to be used in this study due to their accessibility, cost-effectiveness, time effectiveness, simplicity of use, reusability and practical method [14,15]. The utilization of CPS exhibits potential in the elimination of undesired compounds from MK and related pozzolans. This is due to its comparable properties with *Azadirachta indica* bark and other noteworthy biomaterials, as presented in **Table 1**. These biomaterials possess low moisture and high fixed carbon contents, rendering them effective adsorbents for remediation purposes [14].

**Table 1** Proximate properties of some biomaterials [14].

S/No.	Biomaterial	Moisture (%)	Ash (%)	Fixed Carbon (%)
1	<i>Azadirachta Indica</i> bark	3.1	4.5	82.3
2	<i>Carica Papaya</i> stem	3.0	7.4	69.1
3	<i>Moringa Oleifera</i> leaf	8.1	12.7	69.4
4	<i>Camellia sinensis</i> dust	1.9	12.4	73.1

The agricultural biomaterial (i.e., the CPS) and MK are readily available in the country. This will promote waste to wealth policies, proper and agricultural waste management. Efforts are made in this study to use AC from aged and unproductive CPS to remove some unwanted compounds or impurities from MK during or after calcination process of the MK. Thus, it helps to look into effect(s) of AC on chemical properties of MK. MK, which is derived from naturally occurring KC, has been used extensively in place of cement in mortar and concrete manufacture, but not much attention has been paid to considering the effects of the clay source on its pozzolanicity. In addition, the delay in achieving strength of pozzolan mixed concrete requires the use of innovative materials that will improve strength development at an early stage [1]. By the end of this study, it is anticipated that the CPSAC will be able to reduce or remove the undesirable compounds or impurities from MK, leading to the production of MK with less or no impurities, which will promote or improve the development of strength when used in concrete or mortar at an early stage. However, determining the composite's strength qualities is not the study's primary objective.

## Materials and methods

### Materials, equipment and apparatus

This study used CPS, KC and the reagents, which were distilled water and HCl. Equipment used were muffle furnace (5X1-1008 model), oven (Uniscope- SM9053 model), mechanical grinding machine (Controls - EN12390-2 model), Scanning Electron Microscope (SEM - Joel - JSM - 7600F model), Rigaku X-ray diffractometer (Rigaku miniflex and diffraction model), Herzog Gyro-mill (Simatic C7-621 model), XRF equipment (Phillips PW-1800 model), mechanical sieve shaker (Controls - 15DO410 model), sieve and weighing balance. The apparatus employed in the experiment included a crucible, conical flask, beaker, test tubes, dropper, funnel, heating bottle, measuring bottle, heating mantle, paper tape and volumetric flask.

## Methods

### *Development of Carica Papaya Stem Activated Carbon (CPSAC)*

The CPS sample was collected from Federal Polytechnic teaching and research farm, Ado-Ekiti, Nigeria. The coordinates of the sampling point are Latitude 7°59'00" N and Longitude 5°30'00" E. The collected CPS sample was sliced into pieces and then cleaned with distilled water to get rid of dirt and other impurities. It was first air-dried and then dried in an oven (Uniscope model SM9053) at 105°C for 24 h until the weight remained the same. It was then ground using a mechanical grinding machine (Controls - EN12390-2 model).

The resulting powder was sieved to 0.425 mm grain size using a mechanical sieve shaker (Controls - 15DO410 model) for analysis purpose. The powdered CPS samples were carbonized in a muffle furnace (5X1-1008 model) for 2 h at a set temperature of 600 °C, brought out of the furnace, cooled for another 2 h, thereafter, washed with distilled water (3 to 5 times) until they attained a pH of 7.0. After drying in an oven at 105 °C for 2 h, it was then soaked in 0.3 M of activating agent (i.e. reagent - HCl) for 24 h at room temperature (30 °C). Following filtration, the sample underwent continuous washing using a BS Sieve 40 with distilled water until achieving a pH of 7.0. Subsequently, it was subjected to oven drying at a temperature of 105 °C, followed by a cooling period of 2 h. Finally, the sample was stored in vacuum desiccators in preparation for further experimentation. The modified method of [6] was used.

### *Development of Metakaolin (MK)*

KC was collected from Ikere - Ekiti, Nigeria. The coordinates of the sampling point are Latitude 7° 47' 57" N and Longitude 4°29' 03" E. The KC samples obtained were placed in airtight bags and transported to the laboratory. Subsequently, the samples were subjected to air-drying, mechanical grinding, and oven-drying at a temperature of 105 °C for a duration of 24 h until a constant weight was achieved. MK is made by heating the dried KC inside muffle furnace at a temperature of 700 °C up to 2 h and allowed to cool before being kept inside desiccator. The modified method of [6] was used.

### *Treatment of samples*

CPSAC (5, 10, 15, 20 and 25% by weight of KC and MK) was thoroughly mixed with 200 g of each of KC and MK. The KC+CPSAC samples were subjected to calcination inside a muffle furnace at 700 °C and removed after 1 to 2 h then allowed to cool; while the MK+CPSAC samples were soaked in water (125 mL for each sample) for 24 h, thereafter oven-dried at 105 °C. The resulting samples were then characterized.

### *Characterization of samples*

The samples (CPSAC, KC, MK, KC + CPSAC and MK + CPSAC samples) were characterized in order to examine their functional classes (CPSAC only), surface morphology, determine their mineralogical and oxide compositions. Fourier Transform Infra-Red (FTIR) spectroscopic analysis was used to determine the functional classes of the CPSAC. The surface morphology of all the samples was examined using a Scanning Electron Microscope (SEM), and their (except for CPSAC) mineralogical and oxide compositions were determined using XRD and XRF techniques, respectively.

### *FTIR analyses of CPS and CPSAC*

The typical functional classes present on the CPS and CPSAC samples' surface were gotten through FTIR spectroscopic analysis using Infrared Spectrophotometer (Buck Model 530) at Central Research Laboratory, LAUTECH, Ogbomosho, Nigeria. The range of spectra estimated was 4000 to 400 cm<sup>-1</sup> in order to capture the needed functional groups. The dried sample (1 mg) and KBr (500 mg) (Merck, for spectroscopy) were blended in a transparent mortar and subsequently pressed the developed blend at 10,000 Kg cm<sup>-2</sup> for 15 min under vacuum. The resulted FTIR spectra give data on the typical functional groups present on the CPS and CPSAC surfaces, and then compared [14].

### *Surface morphology*

Scanning Electron Microscope (SEM; Joel - JSM - 7600F model), was used to analyse the surface morphology of the samples in accordance with [6]. Selected materials were placed in stubs within a vacuum chamber and the electron beams of the machine were scanned through it to obtain images with a magnification of 10,000 times and a resolution of 120 μm. The SEM images provide information regarding the surface morphology of the selected samples [20].

### *Mineralogical composition*

The basic characterization of material parameters, such as crystal structure, crystallite size and strain is done using XRD. The mineral content of the samples was analyzed using a Rigaku X-ray diffractometer - Rigaku Mini Flex and Diffraction model. Powdered samples were pelletized and then sieved to 0.074 mm. After that, these were placed in a grid made of aluminium alloy measuring 35 mm by 50 mm on a plate of flat glass and covered with paper. The samples underwent compression through the application of minimal manual force while wearing a protective hand covering. After running each sample through the Rigaku X-ray diffractometer (Rigaku mini flex and diffraction model), the instrument was adjusted to generate diffractions within the 2 to 50 degree range at a scanning rate of 2 degrees per minute, while maintaining a radiation setting of 40 kV and 20 mA at room temperature. The diffraction data that was collected (both the d value and the relative intensity) was compared to the standard data of minerals that were found in the mineral powder diffraction file. A similar diffraction pattern indicates the presence of the same minerals as the standard minerals that are found in the sample of soil [6,21,22].

### *Oxides' composition*

The XRF technique uses extra X-rays produced by irradiating a sample to analyze elements qualitatively and quantitatively. It can swiftly and accurately test the elemental makeup of several samples without causing any damage. XRF equipment (Phillips PW-1800 model) was used to determine the oxides' composition of the samples. The pulverization process of each sample was carried out utilizing a Herzog Gyro-mill (Simatic C7-621 model) for duration of 1 min subsequent to its crushing by means of an electric crusher. After pulverizing, 20g of each sample was ground with 400mg of stearic acid for 1 min to make pellets. To prevent blemish, the gyro mill was cleansed after each grinding that was performed. As a binding agent, 1g of stearic acid was measured into an aluminium cup and filled with the sample until it reached the level point. The Herzog pelletizing equipment exerted a force of 200 kN for a duration of 60 s onto the cup, following which 2 mm pellets were deposited into the sample cup of the Phillips PW-1800 XRF instrument. This equipment is based on the principles of quantum chemistry and atomic physics. The specimen's element was quantified using spectral line energies of the emitted lines' wavelengths. Quantitative analysis was performed by correlating the strength of the emitted line to the substance's concentration [6,23].

### *Optimization studies*

The data obtained from chemical composition analyses (XRF analyses) of MK + CPSAC and KC + CPSAC samples were thereafter optimized (Optimal conditions) with Central Composite Design (CCD) in the Response Surface Methodology (RSM) of Design Expert Version 13 (DOEv13) [15-17].

## **Results and discussion**

### **Produced samples**

The samples (i.e. Raw CPS, CPSAC, MK, KC + CPSAC, MK + CPSAC) produced are shown in **Figures 1 - 4**.



**Figure 1** CPS powder and CPSAC.



Figure 2 KC processed into MK.



Figure 3 CPSAC and MK mixed samples (MK + CPSAC).



Figure 4 CPSAC and KC mixed samples (KC + CPSAC).

### Characterization of precursor samples

#### *Functional classes of CPSAC*

The FTIR wavelength amplitudes for the CPS powder and CPSAC are shown in **Figure 5**, and **Table 2** depicted their comparison results. In order to determine where there are changes in IR amplitudes, the CPS powder FTIR wavelength amplitudes were compared with those of CPS. The FTIR spectra showed that few types of amplitude emerged or vanished, but most were moved lower or higher. The change in amplitude values was caused by the formation of chemical bonds between the functional classes of CPS, confirming the possibility of diverse contaminants being adsorbable by CPS with adequate and satisfying removal ability based on the FTIR. The FTIR spectroscopic investigations of the spectra of the 2 adsorbents revealed that the IR amplitudes ranged from 3930.6 to 746.3  $\text{cm}^{-1}$ . While the IR percent reflectance of CPSAC is between 0 and 15, that of the CPS ranges from 0 to 50.

The differences in IR amplitudes between the CPS and CPSAC are displayed in **Table 2**. Bond types become lower at IR amplitudes of 3787.9, 3657.6, 3232.8, 2919.3, 2762.6, 2544.1 and 2470.6  $\text{cm}^{-1}$ . After enhancement, that of 3315.5, 3044.6, 2984.1, 2819.8 and 2614.5  $\text{cm}^{-1}$  went higher. With IR amplitudes of 3480.1, 2702.4 and 2402.4  $\text{cm}^{-1}$ , bond types vanished, whereas those with IR amplitudes of 3708.5, 3604.0, 3536.3 and 2575.5  $\text{cm}^{-1}$  emerged. Bond types become lower at 2282.3, 2228.9, 2119.2, 1767.9, 1675.0 and 1555.2  $\text{cm}^{-1}$ ; then, the values at 1439.1 and 1318.1  $\text{cm}^{-1}$  moved higher. The changes in the FTIR amplitudes demonstrated that CPSAC would be helpful in the elimination or removal of metals, unwanted compounds and oxides from soil and water. Therefore, the changes in the amplitudes supported the effects of enhancement on CPS and in order to improve the functional classes on the adsorbent, enhancement is crucial. According to Wang *et al.* [24] among others, the presence of functional classes in the adsorbent, such as alcohols, aldehydes, amines, carboxylic, esters, lactones, ketones and ether groups, gave it the ability to bind metal ions and oxides by donation of an electron pair from these classes to form complexes with the metal ions in solution. Hence, CPSAC may be able to remove metal ions, oxides and compounds from KC and MK. The CPSAC achieved its capability within short IR amplitudes (i.e. 3930.6 to 747.3  $\text{cm}^{-1}$ ) and percent reflectance (i.e. between 0 and 15). This suggested that CPSAC might be able to absorb metals more effectively.

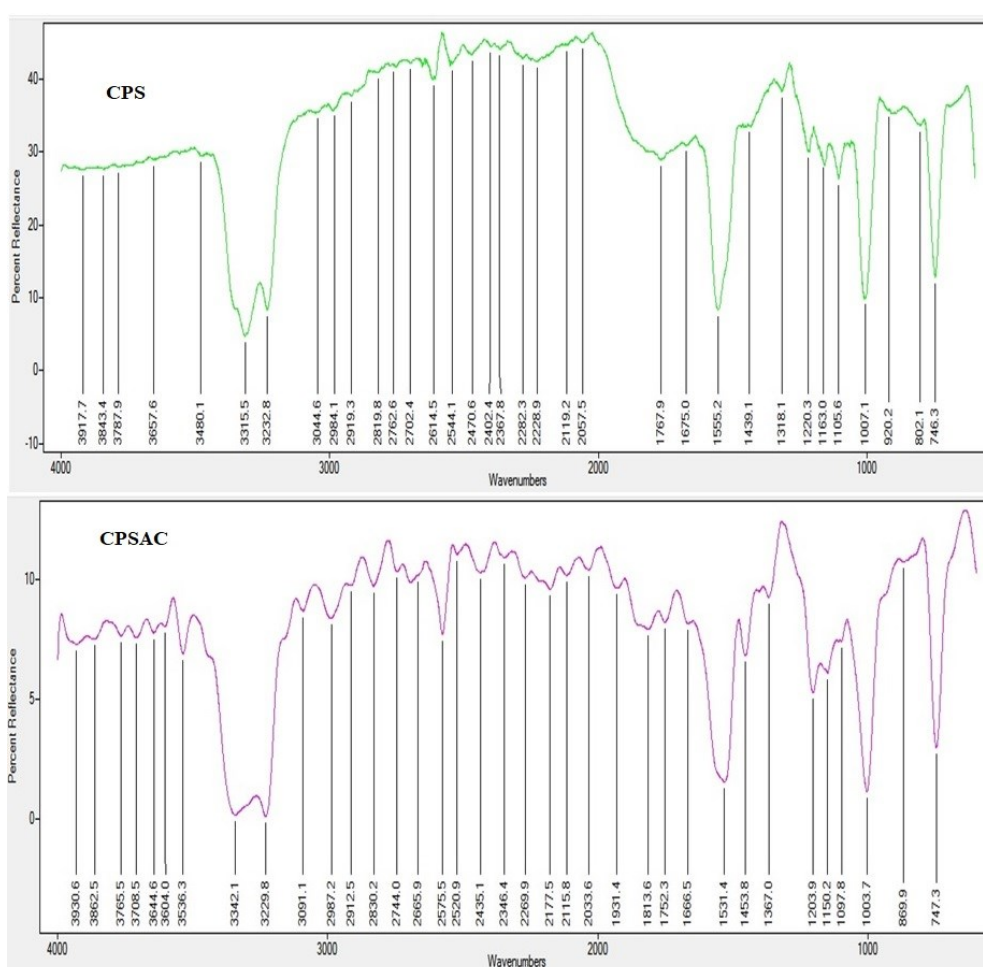


**Figure 5** FTIR wavelength amplitudes for CPS and CPSAC - functional classes.

#### Surface morphology

The surface morphology of CPSAC and MK using SEM are shown in **Figures 6 and 7**. **Figure 6** demonstrates that CPSAC surface was rough and uneven, with numerous pores present. They have numerous pores because of alteration made by the activating agent. Due to the thermal decomposition of lignocelluloses' materials, the CPSAC surface contains rough voids of significant pore structures. Materials with formed pores are typically the result of the evaporation of volatile chemicals. Pores were formed on the precursor as a result of burning off of carbon when the rate of reaction increased during

activation. Since carbon components were lost in the forms of CO and CO<sub>2</sub>, the materials became more porous and new pores were formed. Porous materials were produced due to the physiochemical treatments as expressed by [14].

It is observed from **Figure 6** that MK surface was rough, angular and platy in nature. They have many pores due to the modification as a result of the calcination process. The presence of characteristic kaolinite profiles (“structures”) with dense surfaces and varying dimensions has been confirmed by the studies [2,3]. There was increase in quantity of MK produced with increase in calcination temperature, which promotes the dissolution of kaolinites and generates more gels to bind the quartz powder as supported by [18]. Many large pores were found on the surfaces of the CPSAC (in honey comb shapes) and MK. The findings of this study indicate that the utilization of the activating agent and calcination procedure effectively generated substantial porous surface structures through the creation of multiple and very clear pores on their surfaces. The reaction between CPSAC and MK was enhanced by the porous surfaces.

**Table 2** Changes in the IR amplitudes of the CPS and CPSAC.

CPS			CPSAC		
IR Amplitude	Functional Classes	IR Amplitude	Functional Classes	Remarks	
3917.7		3930.6		Moved higher	
3843.4		3862.5		Moved higher	
3787.9	Alcohols, Phenols and Carboxylic acids	3765.5	Alcohols, Phenols and Carboxylic acids	Moved lower	
		3708.5		Emerged	
3657.6	Alcohols, Phenols and Carboxylic acids	3644.6		Moved lower	
		3604		Emerged	
		3536.3		Emerged	
3480.1	Amides			Vanished	
3315.5	Alcohols, Phenols and Carboxylic acids	3342.1	Alcohols, Phenols and Carboxylic acids	Moved higher	
3232.8		3229.8		Moved lower	
3044.6	Aldehydes, Amides, Carboxylic acids, Ketones & Lactones	3091.1	Aldehydes, Amides, Carboxylic acids, Ketones & Lactones	Moved higher	
2984.1		2987.2		Moved higher	
2919.3		2912.5		Moved lower	
2819.8		2830.2		Moved higher	
2762.6		2744		Moved lower	
2702.4					Vanished
2614.5		2665.9		Aldehydes, Amides, Carboxylic acids, Ketones & Lactones	Moved higher
		2575.5			Emerged
2544.1		2520.9			Moved lower
2470.6		2435.1			Moved lower
2402.4			Vanished		
2367.8		2346.4		Moved lower	
2282.3	Alkynes and Nitrites	2269.9	Alkynes and Nitrites	Moved lower	
2228.9	Alkynes and Nitrites	2177.5	Alkynes and Nitrites	Moved lower	
2119.2	Alkynes and Nitrites	2115.8	Alkynes and Nitrites	Moved lower	
2057.5		2033.6		Moved lower	
		1931.4		Emerged	
		1813.6		Emerged	
1767.9	Aldehydes, Carboxylic acids, Ketones & Lactones	1752.3	Aldehydes, Carboxylic acids, Ketones & Lactones	Moved lower	
1675		1666.5		Moved lower	
1555.2	Amides	1531.4	Amides	Moved lower	
1439.1		1453.8	Amides	Moved higher	
1318.1	Aromatic Amines & primary or secondary OH	1367	Aromatic Amines & primary or secondary OH	Moved higher	
1220.3	Aldehydes,	1203.9	Aldehydes,	Moved lower	

	CPS		CPSAC	Remarks
1163	Carboxylic acids, Ketones & Lactones	1150.2	Carboxylic acids, Ketones & Lactones	Moved lower
1105.6		1097.8		Moved lower
1007.1		1003.7		Moved lower
920.2				Vanished
802.1	Amines	869.9		Moved higher
746.3	Esters	747.3	Esters	Moved higher

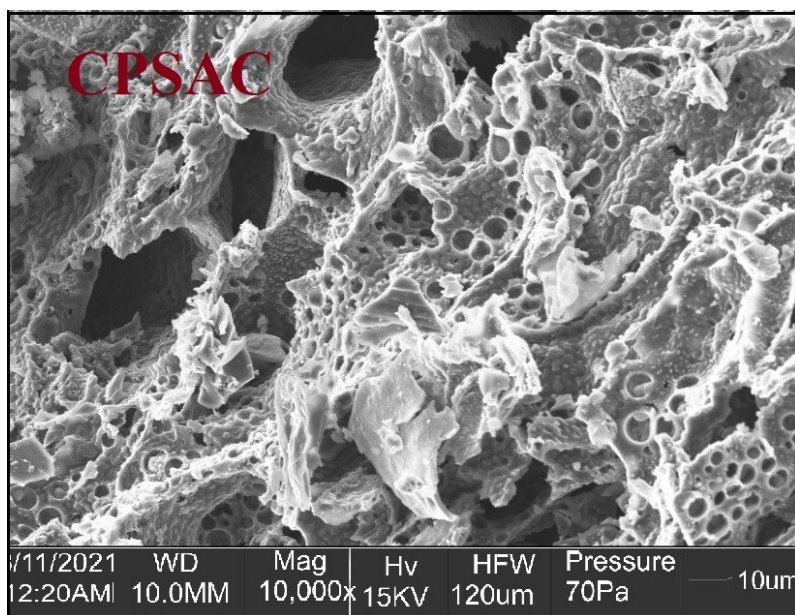


Figure 6 CPSAC SEM - surface morphology (×10,000).

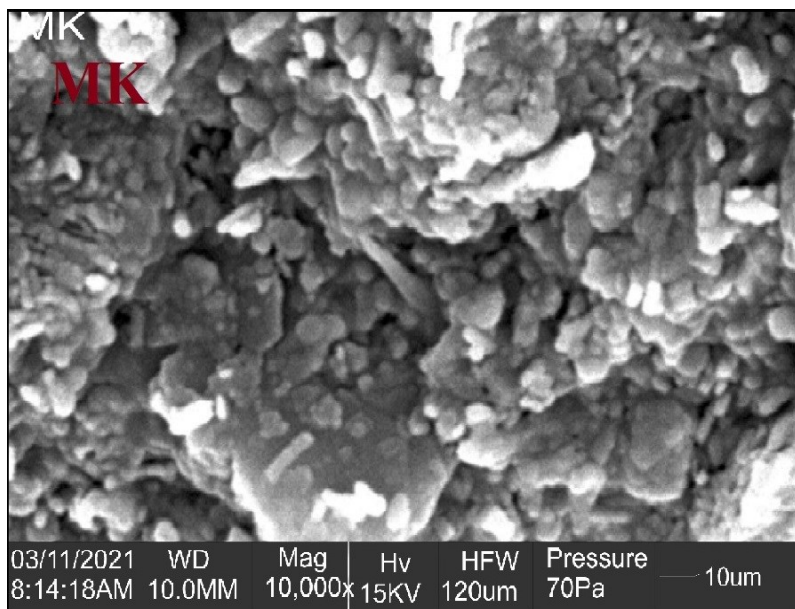
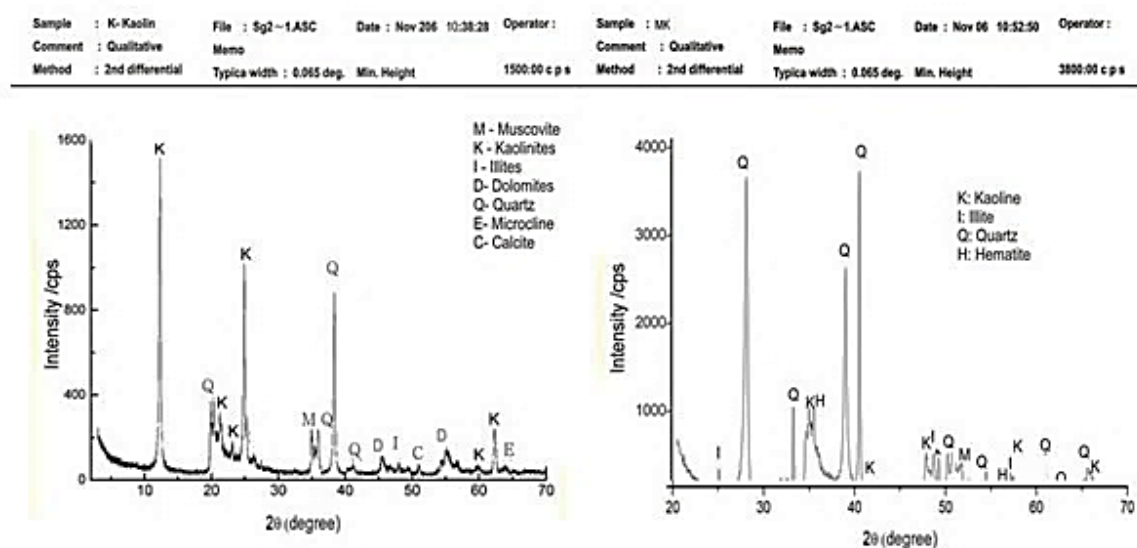


Figure 7 MK SEM - surface morphology (×10,000).

*Mineralogical composition*

**Figure 8** indicate the mineralogical compositions of KC and MK. The peak levels of their performance were analyzed and compared in order to verify the presence of any alterations. The minerals calcite, dolomite, microcline and muscovite underwent disappearance, whereas the mineral hematite underwent appearance. The SEM result (**Figure 7**) was supported by the presence of silica-rich mass, specifically quartz with kaolinite and muscovite, as depicted in **Figure 7**. The XRD patterns confirmed the disappearance of kaolinite pinnacles after calcination, while pinnacle (s) assigned to quartz remains unchanged. These findings are consistent with those of [2,3].

The XRD patterns illustrated in **Figure 8** indicate that the extent of pinnacles of the KC sample varied between 200 and 1600 cycles per second for kaolinite, 200 to 1000 cycles per second for quartz, and below 400 cycles per second for other minerals. In relation to the MK sample, the intensities of quartz peak moved to 4000 cycles per second, whereas the intensities of other minerals remained below 1000 cycles per second. Additionally, there was an increase in the concentration of quartz. In general, the pinnacles exhibited a rise ranging from 1600 to 4000 cycles per second. The observed change in the extent of pinnacle values provides evidence for the impact of calcination on KC, leading to the formation of MK, as previously reported [4].



**Figure 8** Mineralogical composition - XRD intensities of KC and MK.

*Chemical composition*

**Table 3** reveals the chemical compositions of KC and MK. The materials exhibited elevated levels of alumina (Al<sub>2</sub>O<sub>3</sub>) and silica (SiO<sub>2</sub>). The opinions were buttressed by the XRD patterns depicted in **Figure 8**, as well as previous studies conducted by a number of researchers, including [2,5]. Additionally, it was observed that unwanted compounds or oxides (referred to as “others”) were present in KC and persisted in MK post-calcination, albeit in reduced quantities. This suggests the existence of impurities - these are not associated with the kaolinite profile. The XRD analyses presented in **Figure 7** indicate that these compounds have links with hematite, illite and other similar compounds [3,13].

**Table 3** Chemical analyses of KC and MK.

Sample	SiO <sub>2</sub>	Al <sub>2</sub> O <sub>3</sub>	Fe <sub>2</sub> O <sub>3</sub>	CaO	Others	Source
MK	70.2	23.3	1.1	0.02	5.4	This study
MK	57.4	38.6	0.8	0.03	3.2	[2]
MK	50.1	19.2	1.7	4.4	24.6	[5]
MK	54.3	38.3	4.3	0.4	0.8	[11]
MK	55.1	34.1	5.2	0.3	5.3	[19]
KC	58.5	20.5	2.2	2.3	16.6	This study
KC	45.0	39.4	0.8	0.1	14.8	[3]
KC	53.9	29.9	1.8	0.1	14.3	[12]

### CPSAC on MK

**Figure 9** shows CPSAC and MK mixed sample SEM surface morphology. MK + 5, 10 and 15% CPSAC surfaces were rough, angular and platy. The CPSAC produced dense kaolinite profiles (structures) with considerable sizes. The SEM micrograph of MK + 15 % CPSAC showed a conglomeration of the impurities and the kaolinites' structures. The materials become more densified as stipulated by [4]. The presence of numerous pores in the mixtures can be attributed to the change induced by the activating agent. The presence of rough voids on the surface of the mixture's vital pore structures can be attributed to the pyrolytic process of lignocelluloses' materials. Porous materials are typically formed through the process of chemical evaporation with functional properties. A rise in the reaction rate during calcination is expected to lead to the combustion of carbon and the formation of desirable pores on the precursor material. The process of generating porous materials through physiochemical treatments has been stated by [14,18]. The studies of [2,3] depicted the existence of vital kaolinite profiles exhibiting firm surfaces of varying dimensions. The observation of numerous collective pores with significant size on the developed MK surfaces indicates that the CPSAC and calcination procedures were effective in generating high grainy appearance structures, as evidenced by the presence of multiple and very clear pores on their appearances. The grainy appearances facilitated the improvement attempts of the CPSAC on the MK.

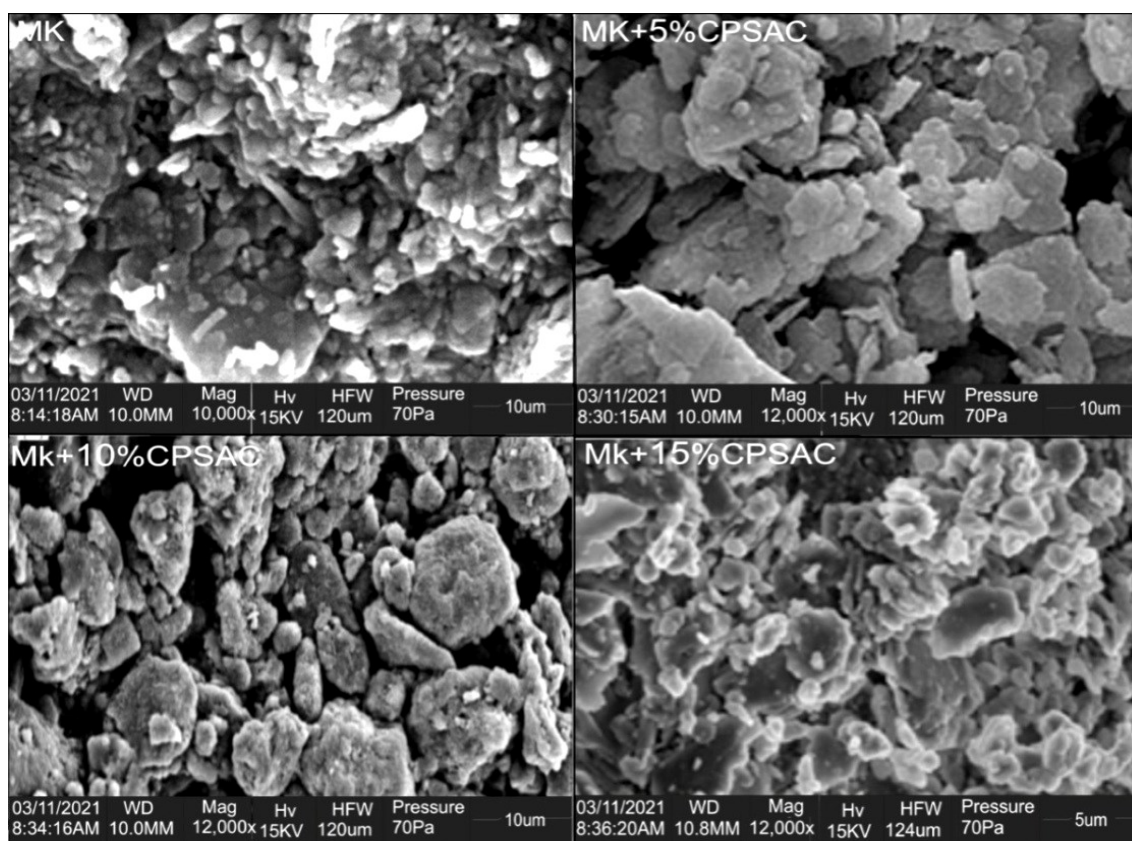


**Figure 9** MK and MK + CPSAC samples SEM surface morphology ( $\times 10,000$ ).

The mineralogical compositions of mixed samples containing CPSAC and MK are depicted in **Figure 10**. The intensity pinnacles were compared to verify the presence of any alterations. The XRD plot for MK + 15% CPSAC demonstrated the reappearance of calcite, dolomite, microcline and muscovite. The SEM result (**Figure 9**) was backed up by the MK + 15% CPSAC XRD plot, which revealed the reappearance of kaolinite, muscovite, and other minerals alongside quartz, which is composed of silica-rich masses.

According to the XRD analyses patterns presented in **Figure 10**, the MK sample exhibited intensity pinnacles ranging from 0 to 4000 cycle per second for quartz, whereas the other minerals displayed values  $< 1000$  cycle per second. The intensities of quartz varied between 200 and 400 cycle per second for samples containing MK + 5% CPSAC, MK + 10% CPSAC and MK + 15% CPSAC. In contrast, the

intensities of other minerals were less than 200 cycle per second. In general, the pinnacles exhibited decrease from 4000 to 400 cycle per second. The observed change in the highest intensity values confirms the impact of incorporating CPSAC into MK. All the samples exhibited non-sharp pinnacles; indicative of crystalline substances being changed into amorphous one. The aforementioned observations were corroborated by the findings of [2,3,18]. The SEM result (Figure 9) was corroborated by the presence of kaolinite, muscovite, and other minerals, along with quartz (aggregates rich in silica), in the XRD analysis pattern of MK + 15% CPSAC.

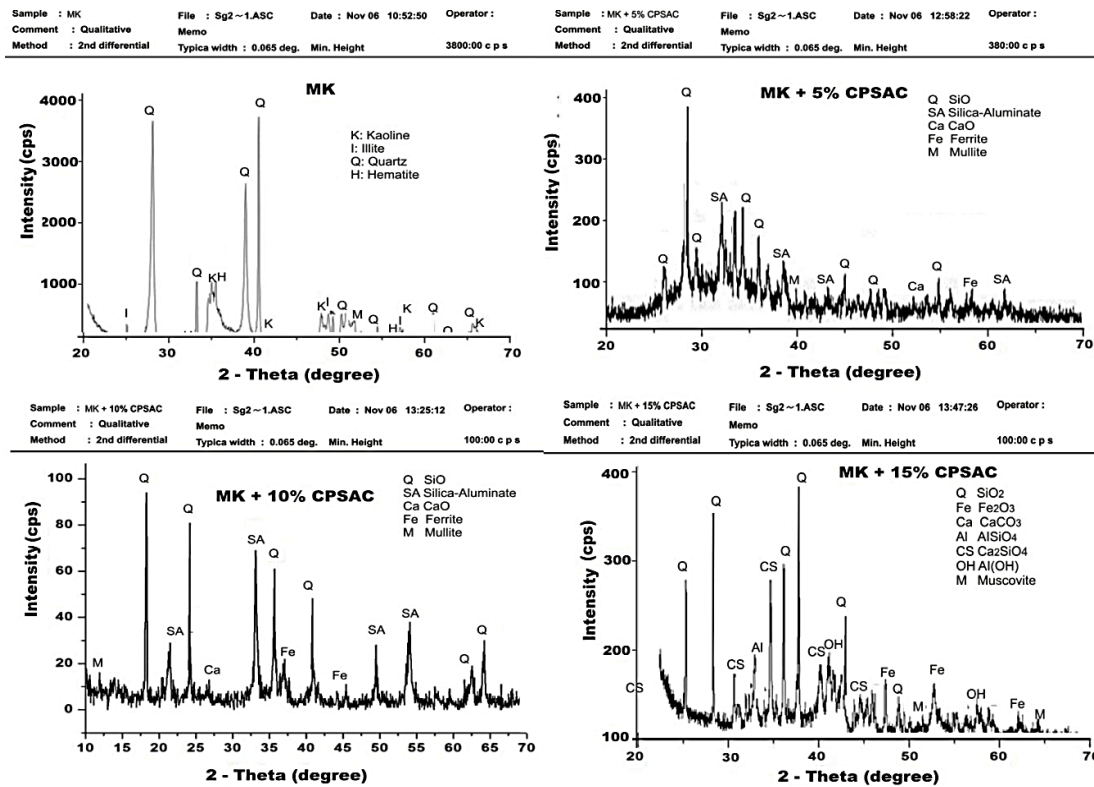


Figure 10 Mineralogical compositions - XRD intensities of MK and MK + CPSAC samples.

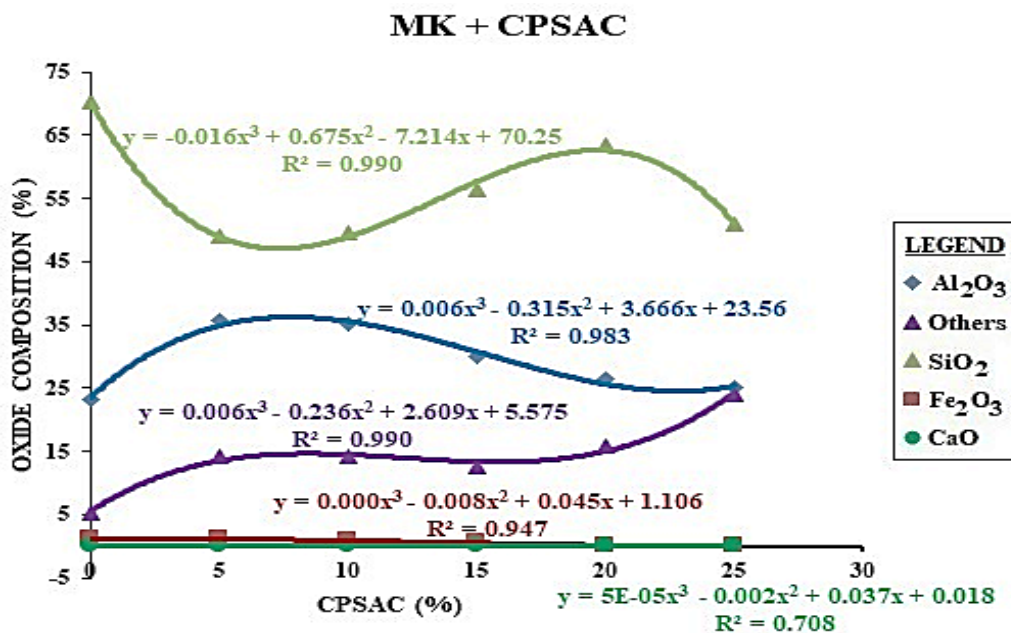


Figure 11 Chemical compositions - graphs of MK oxides compositions against CPSAC.

The graphical representation in **Figure 11** reveals the various oxides' compositions, including  $\text{SiO}_2$ ,  $\text{Al}_2\text{O}_3$ ,  $\text{Fe}_2\text{O}_3$ ,  $\text{CaO}$  and unwanted compounds (referred to as "others"), plotted against CPSAC values ranging from 0 to 25 %. The  $\text{SiO}_2$  content exhibited an initial decline from 0 to 5 % CPSAC content, followed by an increase from 5 to 20 %, and subsequently decreased from 20 to 25 %.  $\text{Al}_2\text{O}_3$  showed an increment from 0 to 7.5 % before declining till it reached 25 % CPSAC. The unwanted compounds (referred to as "others") increased, while  $\text{Fe}_2\text{O}_3$  and  $\text{CaO}$  decreased with an increase in CPSAC content from 0 to 25 %. Though CPSAC removed  $\text{Fe}_2\text{O}_3$ , it also removed important oxide, which is  $\text{CaO}$ , and increase the others (unwanted compounds). Hence, CPSAC has a negative effect(s) when applied directly to MK.

#### Effects of CPSAC on KC

**Figure 12** shows the surface morphology of CPSAC and KC mixed samples using SEM. It is observed that MK + 5, 10 and 15% CPSAC surfaces were rough, angular and platy. They have important kaolinite profiles (i.e. structures) with firm appearances and several sizes as a result of the CPSAC. The kaolinite structures become clearer with the increase in CPSAC content, which may depict the removal of unwanted compounds as the CPSAC content increases. The addition of more CPSAC compacts the microstructure of MK, which might likely result in enhanced mechanical strength, according to an analysis of SEM graphs [4].

The mineralogical compositions of mixture of CPSAC and KC samples are shown in **Figure 13**. Calcite, dolomite, microline and muscovite disappeared in KC + 15% CPSAC, KC + 10 % CPSAC and KC + 15 % CPSAC XRD plots. The simultaneous presence of kaolinite and quartz (aggregates rich in silica) as shown in KC with CPSAC XRD plots supported the SEM results (**Figure 11**). The XRD patterns confirmed the disappearance of kaolinite pinnacles after the addition of CPSAC content, while pinnacle(s) assigned to quartz or  $\text{SiO}_2$  dominated the plot(s). The pinnacles illustrating improvement in the MK made from the CPSAC-KC mix were reported by the XRD patterns.

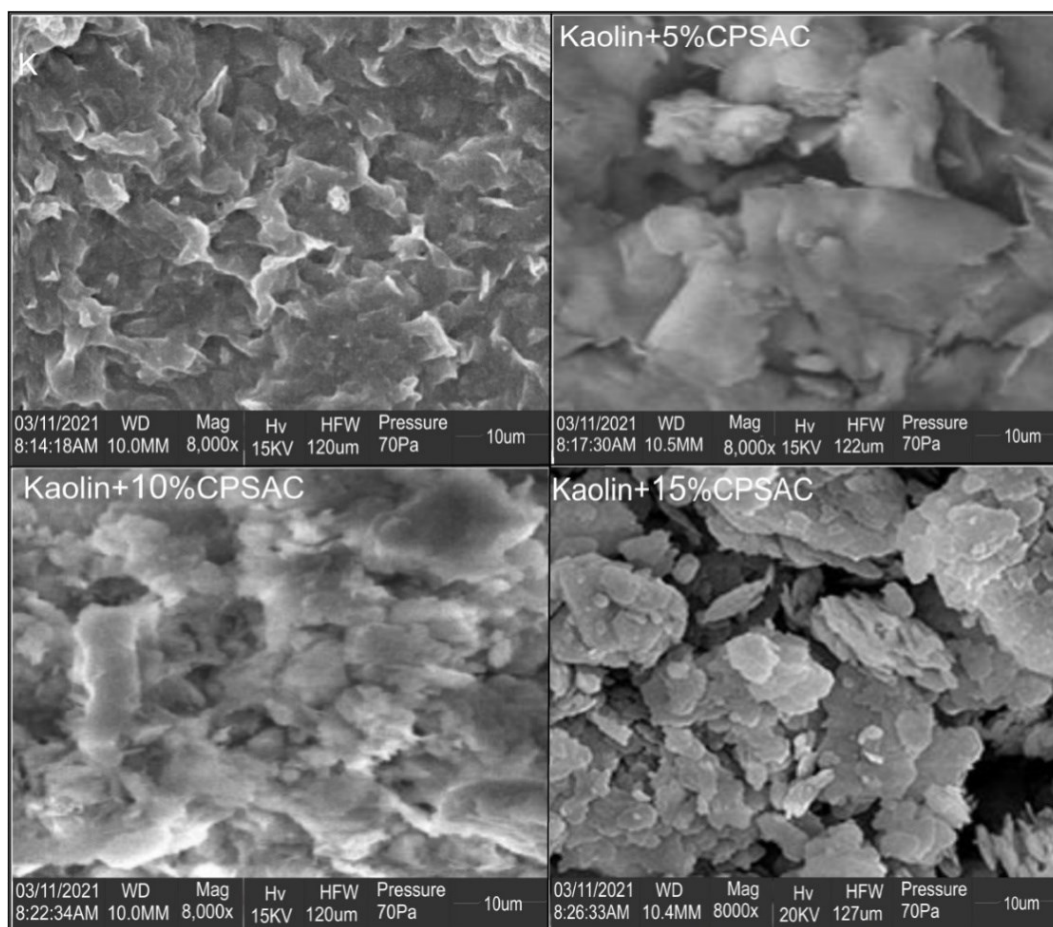


**Figure 12** KC and KC + CPSAC sample SEM surface morphology ( $\times 8000$ ).

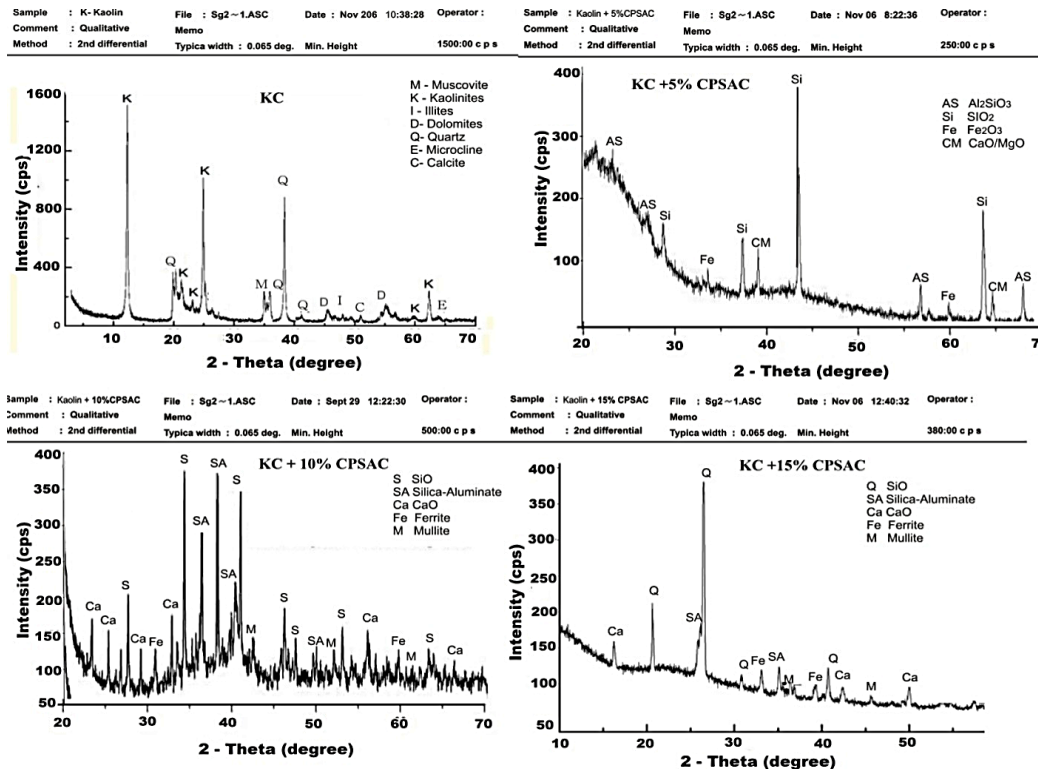


Figure 13 Mineralogical compositions - XRD intensities of KC and KC + CPSAC samples.

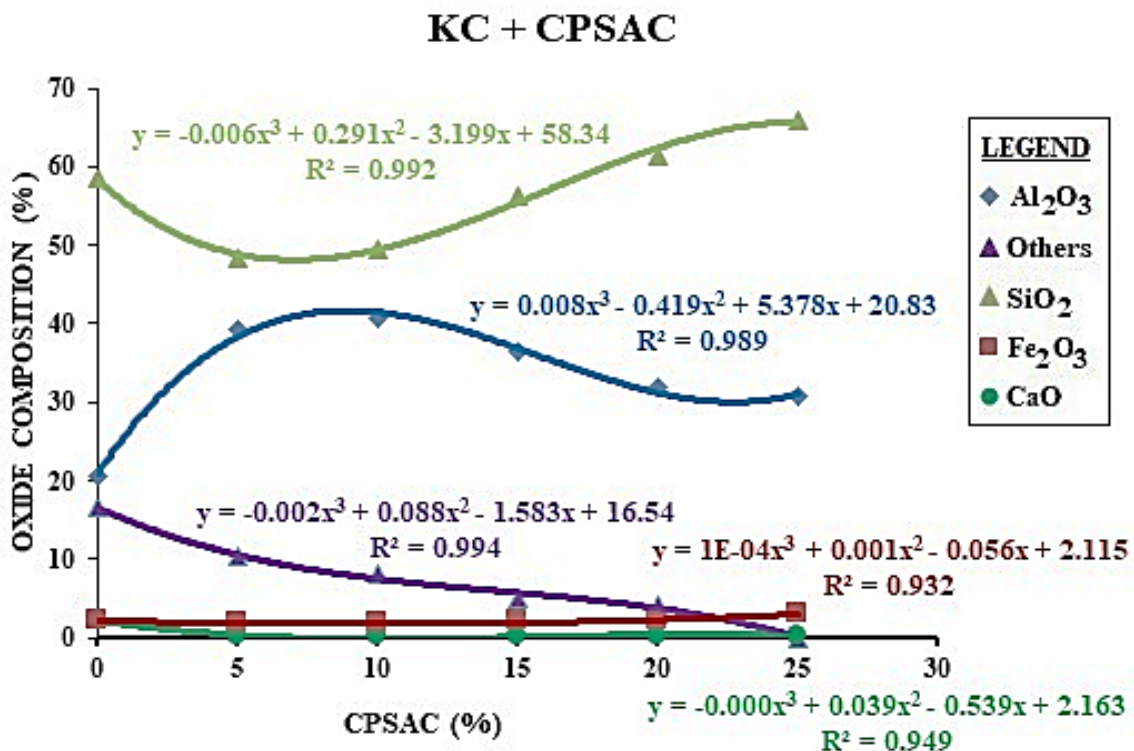
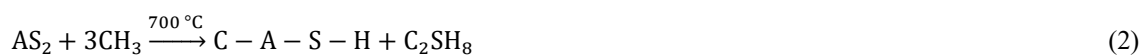
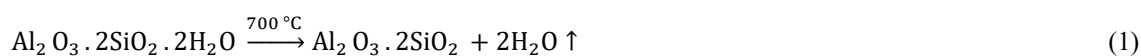


Figure 14 Chemical compositions - graphs of KC oxide compositions against CPSAC.

The KC sample's intensity pinnacles varied between 0 and 1600 cycles per second for kaolinite and quartz as illustrated in the XRD patterns presented in Figure 13, whereas the remaining minerals exhibited values less than 400 cycles per second. The quartz intensity pinnacles varied from 100 to 400

cps for KC specimens blended with CPSAC constituents, whereas the remaining minerals exhibited intensities lower than 200 cycles per second. In general, the pinnacles exhibited decrease from 1600 to 400 cycles per second. The observed change in the maximum intensity values provides evidence for the impact of incorporating CPSAC into KC in the course of calcination. These observations portrayed that the CPSAC content has influence(s) on the production of MK during heat treatment. As a result, there is a propensity to alter the MK's crystalline structure, turning it into an amorphous form and enhancing the pozzolanic potential. The procedure may cause the KC's pores to release bound water atoms, and it may also cause the crystal structure to deform [1,5].

Three distinct stages could be used to express the CPSAC-KC blend's response mechanism. When KC was dehydroxylated to yield alumino-silicate (MK) content, the initial reaction, which was decisive in nature took place, as illustrated in Eq. (1). The MK (AS<sub>2</sub>) then reacted with the CH in the CPSAC to create C-A-S-H (as described in Eq. (2)), adding to the strength of the MK through pore filling. Alumina (A) in MK and fixed carbon(CPSAC) underwent their subsequent reaction to create carbo-aluminate as expressed in Eq. (3). As more carbo-aluminate is created, it contributes to the MK's strengthening and refinement, which improves its reactivity [3,7].



**Figure 14** shows the graphical representation of the compositions of oxides such as SiO<sub>2</sub>, Al<sub>2</sub>O<sub>3</sub>, Fe<sub>2</sub>O<sub>3</sub>, CaO and unwanted compounds (referred to as “others”), against CPSAC values ranging from 0 to 25 %. The SiO<sub>2</sub> and CaO levels exhibited a decline at the onset of 0 to 5 % CPSAC content, followed by a steady rise from 5 to 25 %. Al<sub>2</sub>O<sub>3</sub> showed an initial increment from 0 to 10 % before its decline from 10 to 25 % CPSAC content. Fe<sub>2</sub>O<sub>3</sub> increased with an increase in CPSAC content from 0 to 25 %, while the unwanted compounds (“others”) decreased. These observations demonstrated that CPSAC was able to remove the unwanted compounds (i.e. others) from KC in the course of calcination and not after. It also brought about an increase in significant oxides compositions i.e. SiO<sub>2</sub>, Fe<sub>2</sub>O<sub>3</sub> and CaO. Therefore, CPSAC has a positive effect(s) on MK when applied indirectly (i.e. in the course of the calcination process).

### Optimization studies

Optimization studies conducted on mixed samples of MK+CPSAC and KC+CPSAC to determine the best possible results using design expert software (version 13) indicated that the optimisation solution for the MK + CPSAC sample is 22.05 % of CPSAC, which yielded MK with a composition of 63.89 % SiO<sub>2</sub>, 23.78 % Al<sub>2</sub>O<sub>3</sub>, 0 % Fe<sub>2</sub>O<sub>3</sub>, 0.01 % CaO and 16.40 % of unwanted compounds (“others”) as shown in **Table 3** with standard error of the mean, which falls within the range of 0.20 to 3.37 %. The aftermath was a decrement and increment in Fe<sub>2</sub>O<sub>3</sub> content and unwanted products, respectively. Consequently, there was unwanted compounds increment, removal of significant compounds such as CaO and Fe<sub>2</sub>O<sub>3</sub>, as well as a reduction in one of the major compounds, namely SiO<sub>2</sub> and Al<sub>2</sub>O<sub>3</sub>; however, the remaining major compound (i.e. Al<sub>2</sub>O<sub>3</sub>) was slightly increased.

**Table 4** presents the adverse alterations in compositions of oxides of MK that were made from MK+CPSAC. The percentages of change for SiO<sub>2</sub>, Al<sub>2</sub>O<sub>3</sub>, Fe<sub>2</sub>O<sub>3</sub>, CaO and other compounds were -8.99, +2.06, -100.00, -50.00 and +206.54 %, respectively. The Fe<sub>2</sub>O<sub>3</sub> experienced complete elimination, while there was an undesired increase in unwanted compounds. The optimization solution for the KC+CPSAC sample is 21.42 % CPSAC, which yielded 66.00 % SiO<sub>2</sub>, 29.47 % Al<sub>2</sub>O<sub>3</sub>, 2.29 % Fe<sub>2</sub>O<sub>3</sub>, 2.63 % CaO and 0% unwanted components (“others”) compositions of MK - these depleted unwanted compounds. The standard error (“deviation”) falls within the range of 0.28 to 2.95 %, considerably below the 5 % significant status. This solution verified the percentage of CPSAC that will be blended with KC before being calcined with the aim to create MK devoid of undesirable compounds, and that CPSAC indeed removed undesirable compounds from MK during the calcination process. As indicated in **Table 3**, MK generated from KC+CPSAC had advantageous oxide composition changes of +12.76, +43.76, +6.51, +16.89 and -100.00 % for SiO<sub>2</sub>, Al<sub>2</sub>O<sub>3</sub>, Fe<sub>2</sub>O<sub>3</sub>, CaO and others, respectively, removing and increasing undesired and significant compounds.

**Table 5** shows that the compositions of oxides of MK generated from KC + CPSAC in the course of calcination were better than those of [2,5,6,11,19] and others. MK produced from this study and [6] showed the better production without unwanted compounds. According to Adetoro and Ojoawo [6], 16.22 % of AIBAC was utilized when compared to this study, which used 21.42 %. However, some of the oxides of MK produced from this study have quantities that are higher than that of [6], thus make it better. Moreover, both studies showed the possibilities of using AC produced from agricultural bio-materials in remediating unwanted compounds from MK during calcination process, thus, favourable alterations during MK production.

**Table 4** Alteration in oxide compositions of MK produced.

S/No.	Sample	CPSAC (%)	SiO <sub>2</sub> (%)	Al <sub>2</sub> O <sub>3</sub> (%)	Fe <sub>2</sub> O <sub>3</sub> (%)	CaO (%)	Others (%)	Std. Error (%)
1	MK		70.20	23.30	1.13	0.02	5.35	
2	MK + CPSAC	22.05	63.89	23.78	0.00	0.01	16.40	0.20 - 3.37
3	Alteration		-8.99%	2.06%	-100.00%	-50.00%	206.54%	
4	KC		58.53	20.50	2.15	2.25	16.57	
5	KC + CPSAC	21.42	66.00	29.47	2.29	2.63	0.00	0.28 - 2.95
6	Alteration		12.76%	43.76%	6.51%	16.89%	-100.00%	

Note: Alterations in (S/No. 3) were calculated using  $[(MK+CPSAC) - (MK) \times 100\% / MK]$ ; while that of (S/No. 6) were calculated using  $[(KC+CPSAC) - (KC) \times 100\% / KC]$ .

**Table 5** Oxide compositions of MK.

Sample	SiO <sub>2</sub>	Al <sub>2</sub> O <sub>3</sub>	Fe <sub>2</sub> O <sub>3</sub>	CaO	Others	Source
MK	66.00	29.47	2.29	2.63	0.00	This study
MK	50.10	19.20	1.74	4.42	24.55	[5]
MK	57.37	38.63	0.77	0.03	3.20	[2]
MK	55.10	34.10	5.24	0.28	5.28	[19]
MK	54.30	38.30	4.28	0.39	0.80	[11]
MK	60.05	33.62	2.22	2.61	0.00	[6]

This study suggests that mixing a specific proportion of CPSAC and/or other suitable agricultural adsorbents with KC before calcining the mixed sample is the key measurable requirement for improved yields of MK. This will promote the removal of unwanted compounds and improve the reactivity of the MK that would be produced by the heating treatment process. Essentially, for KC to be properly transformed into a MK form, it must be properly grilled, pure and never burned. During heat treatment, MK, a silica-based substance, interacts with Ca(OH)<sub>2</sub> to create CSH gel. Additionally, it has alumina that interacts with CH to form the alumina-containing phases C<sub>4</sub>AH<sub>13</sub>, C<sub>2</sub>ASH<sub>8</sub> and C<sub>3</sub>AH<sub>6</sub> [2,3]. With benefits of high reactivity and rate of hydration due to particle packing as shown in **Figure 11**, the MK produced from the CPSAC-KC blend during calcination process is free of impurities or unwanted compounds, which results in stronger and finishing of concrete and mortar with a potential for efflorescence when used. The MK that is generated is considerably different from other types of pozzolans in that CPSAC cleansed it during calcination to improve its colour, particle size and greatly increasing the reactivity. When compared to other alumino-silicate sources (such as fly ash, rice husk ash, etc.), its high reactivity will also make it an ideal component in geo-polymer mortar and concrete for boosting geo-polymerization [1,4,5].

## Conclusions

This study involved the production of AC from CPS through the utilization of an activating agent, namely HCl, and MK from KC by means of calcination. These alterations were successful in developing pores on the surfaces of the precursors, leading to large porous CPSAC and MK. These pores provided

good surfaces for the reaction between CPSAC and MK compounds. The observed changes in pinnacle intensities ranging from 4000 to 400 cycles per second provide evidence for the impact in the course of calcination on the transformation of KC into MK. Unwanted compounds were detected in KC and persisted in MK even in post-calcination, albeit in reduced amounts. The effects of CPSAC on MK were primarily observed in the course of the calcination rather than post-calcination. The 21 and 42% of CPSAC completely removed the unwanted compounds and elements (i.e.  $P_2O_5$ ,  $K_2O$ ,  $TiO_2$ ,  $SO_3$ ,  $Na_2O$ , Cr, Ni, Zn, Cu and Ba) from MK in the course of the calcination process and increased the amount of  $Al_2O_3$ , CaO,  $SiO_2$  and  $Fe_2O_3$  contents by 43.76, 16.89, 12.76 and 6.51 % respectively. The optimum values attained were 66.00% of  $SiO_2$ , 29.47% of  $Al_2O_3$ , 2.29 % of  $Fe_2O_3$  and 2.63 % of CaO compositions of MK. Based on the above findings, CPSAC showed potential as a viable industrial treatment material for environmental friendly MK (an alternative resource to cement) during its production. The potential for applicability of varying calcination temperature, organic acids and bases should be explored for future studies. Application of other agricultural adsorbents for this purpose should also be studied. In order to examine the strength characteristics of the MK from this study in comparison to other pozzolans and MK produced without CPSAC augmentation, further studies should be conducted on its application in the manufacturing of concrete and mortar.

### Acknowledgements

The authors wish to acknowledge the laboratory assistance rendered by the Department of Civil Engineering of the Federal Polytechnic, Ado-ekiti and Ladoke Akintola University of Technology, Ogbomoso, Nigeria.

### References

- [1] AA Raheem, R Abdulwahab and MA Kareem. Incorporation of metakaolin and nanosilica in blended cement mortar and concrete - A review. *J. Cleaner Prod.* 2021; **290**, 125852.
- [2] DL Pillay, OB Olalusi, PO Awoyera, C Rondon, AM Echeverria and JT Kolawole. A review of the engineering properties of metakaolin based concrete: Towards combatting chloride attack in coastal/marine structures. *Adv. Civ. Eng.* 2020; **2020**, 8880974.
- [3] I Sánchez, IS Soto, M Casas, RVDL Villa and R García-Giménez. Evolution of metakaolin thermal and chemical activation from natural kaolin. *Minerals* 2020; **10**, 534.
- [4] BB Jindal, T Alomayri, A Hasan and CR Kaze. Geopolymer concrete with metakaolin for sustainability: A comprehensive review on raw material's properties, synthesis, performance, and potential application. *Environ. Sci. Pollut. Res.* 2022; **30**, 25299-324.
- [5] R Abdulwahab, SO Odeyemi, HT Alao and TA Salaudeen. Effect of metakaolin and treated rice husk ash on compressive strength of concrete. *Res. Eng. Struct. Mater.* 2021; **7**, 199-209.
- [6] EA Adetoro, R Abdulwahab, OD Adetoro, SO Ojoawo and P Naik. Treatment effect on reactivity of metakaolin using *Azadirachta indica* bark activated carbon. *Mater. Today Proc.* 2023; **88**, 119-27.
- [7] F Zunino and K Scrivener. The reaction between metakaolin and limestone and its effect in porosity refinement and mechanical properties. *Cement Concr. Res.* 2021; **140**, 106307.
- [8] MA Keerio, A Saad, A Kumar, N Bheel and K Ali. Effect of local metakaolin developed from natural material soorh and coal bottom ash on fresh, hardened properties and embodied carbon of self-compacting concrete. *Environ. Sci. Pollut. Res.* 2021; **28**, 60000-18.
- [9] HM Hamada, BA Tayeh, A Al-Attar, FM Yahaya, K Muthusamy and AM Humada. The present state of the use of eggshell powder in concrete: A review. *J. Build. Eng.* 2020; **32**, 101583.
- [10] N Bheel, MOA Ali, T Tafsirojjaman, SH Khahro and MA Keerio. Experimental study on fresh, mechanical properties and embodied carbon of concrete blended with sugarcane bagasse ash, metakaolin, and millet husk ash as ternary cementitious material. *Environ. Sci. Pollut. Res.* 2022; **29**, 2554-39.
- [11] TJ Afolayan, OA Adetoye and A Sani. A review on the effect of pozzolanic properties of metakaolin in concrete. *Int. J. Res. Publ. Rev.* 2022; **3**, 1383-8.
- [12] GL Thankam and NT Renganathan. Ideal supplementing cementing material - Metakaolin: A review. *Int. Rev. Appl. Sci. Eng.* 2020; **11**, 58-65.
- [13] KM Ibrahim, MK Moumani and SK Mohammad. Extraction of  $\gamma$ -alumina from low-cost kaolin. *Resources* 2018; **7**, 63.
- [14] EA Adetoro, SO Ojoawo and AM Salman. Adsorption and desorption studies of *Carica papaya* stem activated with zinc chloride in mining wastewater treatment. *Water SA* 2022; **48**, 187-98.

- [15] AE Adetoro and SO Ojoawo. Optimization study of biosorption of toxic metals from mining wastewater using *Azadirachta indica* bark. *Water Sci. Tech.* 2020; **82**, 887-904.
- [16] X Bai, S Wen, J Liu and Y Lin. Response surface methodology for optimization of copper leaching from refractory flotation tailings. *Minerals* 2018; **8**, 165.
- [17] Stat Ease.Design expert software version 13, Available at: <http://www.statease.com>, accessed November2022.
- [18] YO Abiodun, JI Orisaleye and SO Adeosun. Effect of calcination temperatures of kaolin on compressive and flexural strengths of Metakaolin concrete. *Niger. J. Tech. Dev.*2023; **20**, 33-43.
- [19] O Burciaga-Diaz andJI Escalante-Garcia. Structural transition to well-ordered phases of NaOH-activated slag-metakaolin cements aged by 6 years. *Cement Concr. Res.*2022; **156**, 106791.
- [20] A Pallares-Rusiñol, M Bernuz, SL Moura, C Fernández-Senac, R Rossi, M Marti and MIPividon. Advances in exosome analysis.*Adv. Clin. Chem.*2023; **112**, 69-117.
- [21] N Raval, R Maheshwari, D Kalyane, SR Youngren-Ortiz, MB Chougule and RK Tekade. *Importance of physicochemical characterization of nanoparticles in pharmaceutical product development.* In: Basic fundamentals of drug delivery. Academic Press, Cambridge, 2019, p. 369-400.
- [22] E Nossol, RAA Muñoz, EM Richter, PHDS Borges, SC Silva and DP Rocha. Sensing materials: Graphene. *Encyclopedia Sensor. Biosens.* 2023; **2**, 367-88.
- [23] YJ Choi and K Sawada. Physical sensors: Fluorescence sensors. *Encyclopedia Sensor. Biosens.* 2023; **1**, 1-19.
- [24] Q Wang, Y Wang, Z Yang, W Han, L Yuan, L Zhang and X Huang. Efficient removal of Pb(II) and Cd(II) from aqueous solutions by mango seed biosorbent. *Chem. Eng. J. Adv.* 2022; **11**, 100295.